Biogeosciences Discuss., 8, 857–884, 2011
www.biogeosciences-discuss.net/8/857/2011/
doi:10.5194/bgd-8-857-2011

Biogeosciences Discussions

Decreased calcification affects photosynthetic responses of *Emiliania huxleyi* exposed to UV radiation and elevated temperature

K. Xu[1], K. Gao[1], V. E. Villafañe[2], and E. W. Helbling[2]

[1]State Key Laboratory of Marine Environmental Science, Xiamen University, Xiamen, 361005, China
[2]Estación de Fotobiología Playa Unión and Consejo Nacional de Investigaciones Científicas y Técnicas (CONICET) Casilla de Correos No. 15 (9103) Rawson, Chubut, Argentina

Received: 2 January 2011 – Accepted: 17 January 2011 – Published: 1 February 2011

Correspondence to: K. Gao (ksgao@xmu.edu.cn)

Published by Copernicus Publications on behalf of the European Geosciences Union.

Abstract

Changes in calcification of coccolithophores may affect their photosynthetic responses to both, ultraviolet radiation (UVR, 280–400 nm) and temperature. We operated semi-continuous cultures of *Emiliania huxleyi* (strain CS-369) at reduced (0.1 mM, LCa) and ambient (10 mM, HCa) Ca^{2+} concentrations and, after 148 generations, we exposed cells to six radiation treatments (>280, >295, >305, >320, >350 and >395 nm by using Schott filters) and two temperatures (20 and 25 °C) to examine photosynthesis and calcification responses. Overall, our study has demonstrated that: (1) decreased calcification resulted in a down regulation of photoprotective mechanisms (i.e., as estimated via non-photochemical quenching, NPQ), pigment contents and photosynthetic carbon fixation; (2) Calcification (C) and photosynthesis (P) (as well as their ratio) have different responses related to UVR with cells grown under the high Ca^{2+} concentration having a better performance as compared to those grown under the low Ca^{2+} level; (3) elevated temperature increased photosynthesis and calcification of *E. huxleyi* grown at high Ca^{2+} concentrations whereas the opposite was observed in low Ca^{2+} grown cells. Therefore, a decrease in calcification rates in *E. huxleyi* is expected to decrease photosynthesis rates and producing also a negative feedback, further reducing calcification.

1 Introduction

Coccolithophores are organisms capable of fixing inorganic carbon into organic matter via photosynthesis as well as calcium carbonate crystals via intracellular calcification. In addition to their role as primary producers, coccolithophores play a predominant function in global ocean calcification (Rost and Riebesell, 2004), accounting for up to half of the share (Milliman, 1993). While still there is no a general consensus, calcification in coccolithophores appears to be strongly linked to photosynthesis by favoring supply of CO_2 (Anning, 1996; Sikes et al., 1980; Sikes and Wilbur, 1982); moreover, Nimer (1996) found reduced photosynthetic rates when removing external calcium.

BGD
8, 857–884, 2011

Other studies (Herfort et al., 2002, 2004; Trimborn et al., 2007; Leonardos et al. 2009), however, showed that changes in calcification under altered Ca^{2+} concentrations did not bring about concomitant changes in photosynthesis.

Calcification of coccolithophores is known to be influenced by many factors, such as light availability, nutrients, trace metals and CO_2 as well as temperature (Paasche, 2002; Shiraiwa, 2003; Zondervan, 2007) and ultraviolet radiation (UVR, 280–400 nm) (Gao et al., 2009; Guan and Gao, 2010). Under a scenario of global climate change, important changes in the physiology of diverse aquatic organisms are expected (Beardall et al., 2009), especially due to variations in UVR and temperature levels. In this sense, it has been found that UVR strongly influences photosynthesis and calcification of *Emiliania huxleyi* under CO_2-induced ocean acidification (Gao et al., 2009). In regard to the effects of future ocean warming on coccolithophores, the results are rather varied: on the one hand, it was determined that photosynthesis could be promoted by increases in both pCO_2 and temperature (Feng et al., 2008) but, on the other hand, De Bodt et al. (2010) suggested that ocean acidification has a larger adverse impact than surface water warming on coccolithophorids' calcification.

Emiliania huxleyi (Lohmann) W. W. Hay and H. P. Mohler is a cosmopolitan species that frequently form blooms in shallow-mixed surface oceanic waters with high light exposures (Nanninga and Tyrrell, 1996). This species is therefore of key ecological importance and constitutes an excellent model to evaluate physiological responses under variable environmental stressors i.e., as occurring due to global change. In particular, it has been found that growth and photosynthesis of *E. huxleyi* are very sensitive to UVR (Buma et al., 2000; Guan and Gao, 2010); furthermore, enhanced acidification of seawater exacerbated detrimental UVR effects on this latter process (Gao et al., 2009). In the present study, and considering a context of global change, we further asked whether variations in calcification rates in *E. huxleyi* alter its photosynthetic responses to both UVR and temperature. The experimental approach was to incubate low- and high Ca^{2+} acclimated *E. huxleyi* cells to different radiation conditions (using an artificial source) and temperatures treatments (20 and 25 °C) to determine the

BGD
8, 857–884, 2011

energy-dependant responses (i.e., biological weighting functions, BWFs) of both photosynthesis and calcification.

2 Materials and methods

2.1 Organism and culture conditions

A coccolith-bearing strain of *Emiliania huxleyi* (CS-369) was obtained from the Commonwealth Scientific and Industrial Research Organisation (CSIRO, Australia). The cells were grown in artificial seawater enriched with 100 µM nitrate and 6.25 µM phosphate and with trace metals and vitamins as specified for the Aquil medium (Sunda et al., 2005). Two calcium concentrations were used in our experiments – adjusted to 0.1 mM (LCa) and 10 mM (HCa) by adding $CaCl_2$ – representing the reduced and ambient Ca^{2+} concentration of seawater, respectively. Ecologically, the reduced level of Ca^{2+} may be expected during coccolithorphore blooms where salinity is approximately half the average oceanic value of ~35 (Cokacar et al., 2001); physiologically, reduced Ca^{2+} availability is an effective way to investigate the role of calcification (Brownlee et al., 1995). Semi-continuous cultures were maintained at 20 °C at a PAR level of 150 µmol photons m^{-2} s^{-1} (12L:12D). The media (i.e., LCa and HCa) were renewed every 3 days, and cell concentrations were always kept $< 10^5$ cells mL^{-1}. The cells were grown for at least 100 days (> 148 generations) before being used in the experiments as described below.

2.2 Experimentation

For the determination of the energy-dependant responses (BWFs, biological weighting functions) of photosynthesis and calcification, six different radiation treatments were established by using Schott cut-off filters that cut radiation above 280, 295, 305, 320, 350 and 395 nm (the transmission spectra of these filters have been published

BGD
8, 857–884, 2011

elsewhere, Villafañe et al., 2003). For each experimental Ca^{2+} concentration, the samples were dispensed in six quartz tubes (14 mL) per radiation treatment (i.e., under each Schott filter). Thus a total of 36 tubes were irradiated; half of them were used for measurements of photosynthetic carbon fixation and calcification whereas the other half was used for PAM measurements (see below). The tubes containing the samples were put in a water bath for temperature control using a circulating cooler (CTP-3000, Eyela, Tokyo, Japan) and exposed to artificial radiation under a solar simulator (Sol 1200 W; Dr. Hönle, Martinsried, Germany) at 20 °C or 25 °C for 2 h. The irradiances levels used were 63.5 W m^{-2} (290 µmol photons m^{-2} s^{-1}), 23.1 W m^{-2} and 1.20 W m^{-2}, for PAR, UV-A and UV-B, respectively. The irradiances were measured with a broadband ELDONET filter radiometer (Real Time Computers, Möhrendorf, Germany).

2.3 Analyses and measurements

pH was measured with a potentiometric titrator (DL15, Mettler-Toledo, Schwerzenbach, Switzerland) which was calibrated against Standard National Bureau of Standards (NBS) buffer solution (Hanna). The alkalinity of the media were also measured with the potentiometric titrator. The carbonate system was calculated from temperature, salinity, pH and concentrations of total alkalinity and phosphate, using the program CO_2sys (Lewis and Wallace, 1998). Equilibrium constants of Mehrbach et al. (1973) modified by Dickson and Millero (1987) were chosen for the calculations.

Just before experimentation, samples were taken for determination of pigments and quantification of cells. Cell densities were determined using a Coulter counter (Z2, Beckman Instruments, Florida, US) and specific growth rate was calculated as:

$$\mu = (\ln N_t - \ln N_0)/\Delta t,$$

where N_0 and N_t are the cell concentrations after and before renewing medium.

For pigments determination, 100 mL of sample was filtered onto Whatman GF/F filters (25 mm) under low pressure (200 mbar) and extracted overnight either in absolute

BGD
8, 857–884, 2011

methanol (for chlorophyll-*a* (chl-*a*) determinations) or 90% acetone (for carotenoids content) at 4 °C. After extraction and centrifugation (10 min at 5000 × g) the absorbance of the supernatant was determined with a scanning spectrophotometer (DU800, Beckman, Fullerton, California, USA). The chl-*a* content was calculated according to Porra (2002) whereas that of carotenoids using the equations of Strickland and Parsons (1972). In addition, an aliquot of 10 mL of culture (both from the HCa and LCa treatments) was filtered very gently onto 0.22 µm MCE (Mixed Cellulose Ester) filters (Xinya Instrument Co., Shanghai, China), washed three times with 0.2 M phosphate buffer (pH = 8) and then dried at 45 °C. The filters were coated with gold and then examined with a scanning electron microscope (Field Emission SEM, LEO 1530, Germany).

Fluorescence measurements were performed at 40, 80 and 120 min since the beginning of the incubations. Fluorescence parameters were determined with a pulse amplitude modulated fluorometer (model Xe-PAM, Walz, Effeltrich, Germany). The effective photochemical quantum yield of PSII (Y) was determined by measuring the instant maximal fluorescence (F'_m) and the steady state fluorescence (F_t) of light adapted cells using a saturating white light pulse (5000 µmol photons m^{-2} s^{-1} in 0.8 s) in the presence of a weak measuring light (0.3 µmol photons m^{-2} s^{-1}) and actinic light (300 µmol photons m^{-2} s^{-1}, i.e., similar PAR level as under the radiation treatments). *Y* was estimated according to Genty et al. (1989) as:

$$Y = (F'_m - F_t)/F'_m \quad (1)$$

UVR-induced inhibition of *Y* was calculated as:

$$\mathrm{Inh}(\%) = (Y_{395} - Y_{320/280}) \times Y_{395}^{-1} \times 100 \quad (2)$$

where Y_{395} represents the yield under the PAR (395–700 nm) treatment, while $Y_{320/280}$ represents the Yield under the PA (320–700 nm) or PAB (280–700 nm) treatments, respectively. Non-photochemical quenching (NPQ) was calculated as:

$$\mathrm{NPQ} = (F_m - F'_m)/F'_m \quad (3)$$

BGD
8, 857–884, 2011

where the F_m represents the maximum fluorescence yield after 10 min of dark adaptation.

For measurements of photosynthesis and calcification, samples (i.e., from the HCa and LCa treatments) were dispensed into 14 mL quartz tubes and inoculated with 100 µL – 10 µCi (0.37 MBq) of $NaH^{14}CO_3$ (ICN Radiochemicals, Irvine, California, USA). After incubating for 2 h, sub-samples for total (5 mL) and organic (5 mL) carbon were collected onto Whatman GF/F glass fiber filters (25 mm) under low pressure (200 mbar), rinsed three times with the medium and put in 20 mL scintillation vials. For the determination of organic carbon, the filters were exposed to HCl fumes overnight and dried at 45 °C; then they were digested in scintillation cocktail (Hisafe 3, Perkin-Elmer, Shelton, CT, USA) and the activity of the fixed radiocarbon counted with a scintillation counter (Tri-Carb 2800TR, Perkin-Elmer, Shelton, CT, USA). The calcification rate was calculated as the difference between total (non acidified filters) and organic particulate carbon fixation (acidified filters) as previously reported (Gao et al., 2009; Guan and Gao, 2010).

Biological weighting functions (BWFs) for inhibition of Y, NPQ, photosynthetic carbon fixation and calcification were calculated using an exposure-response curve based on irradiance (Neale and Kieber, 2000). The biological responses for each wavelength interval over the incubation period were expressed as a function of the average irradiance (over incubation time) in the exposure wavelength interval. The relative spectral emission of the solar simulator was determined using a USB diode array spectroradiometer (HR 2000CG-UV-NIR, Ocean Optics, Duneclin, USA). An exponential decay function (base 10) was used to fit the data in each experiment, and the exponent of the function was expressed as a two-degree polynomial function; the best fit was then obtained by iteration ($r^2 > 0.95$).

Data were analyzed using the SPSS v.16.0 software. Interactive effects among Ca^{2+} concentration, temperature, radiation treatments and exposure time on Y, NPQ, photosynthetic carbon fixation (P), calcification rate (C) and C/P were statistically analyzed using a two, three or four-way ANOVA test to establish significance ($p < 0.05$) among

BGD
8, 857–884, 2011

the variables. The Student Newman-Keuls (SNK) test with a level of significance set at $p < 0.05$ was used for post-hoc comparisons. The Student's t-test was also used to analyze growth rates and pigments data.

3 Results

3.1 Carbonate chemistry, growth rates, pigments and morphology

The parameters for the carbonate system of the media are presented in Table 1. Total alkalinity (TA) and CO_3^{2-} concentration were significantly different, with higher TA and CO_3^{2-} levels in the HCa medium. All other parameters did not show significant differences between the two media. After 3 days of culturing and prior to the renewal of media, the pH in both treatments increased to < 0.07; the other parameters did not show significant differences among the two Ca^{2+} treatments.

During the acclimation period, reduced Ca^{2+} concentration did not significantly affect growth rates, but it significantly decreased ($p < 0.05$) the chl-*a* and carotenoids contents by 26.7% and 20%, respectively (Table 2). The SEM images showed no coccolith-covered surface in cells grown at LCa, and furthermore, the coccoliths were partially dissolved and malformed (Fig. 1a). Instead, cells grown at HCa showed entire and strongly calcified coccoliths (Fig. 1b).

3.2 Chl-*a* fluorescence parameters

The main feature of chl-*a* fluorescence parameters was of Y being significantly lower ($p < 0.05$) when samples were exposed to shorter UVR wavebands – i.e., the lowest Y was determined in the 280–700 nm range whereas the highest was in the 400–700 nm (Fig. 2). Additionally, and at 20 °C, significantly higher ($p < 0.05$) Y values were determined in the HCa as compared to the LCa treatment. Furthermore, at 20 °C, increased exposure time significantly decreased ($p < 0.05$) the Y differences among

BGD
8, 857–884, 2011

Ca^{2+} treatments, so that at 40 (Fig. 2a) and 80 min of exposure (Fig. 2b), and for all radiation treatments, Y values were significantly higher ($p < 0.05$) under the HCa than under LCa treatment, but they were similar ($p = 0.06$) after 2 h (Fig. 2c). There was a significant effect of temperature (as seen in the ratio of Y at the two tested temperatures) with samples in the LCa treatments having significantly higher ($p < 0.05$) Y values at 25 °C than at 20 °C when incubated during 40 (Fig. 2a) and 80 min (Fig. 2b), while there were no differences after 2 h of incubation (Fig. 2c). In contrast, samples in the HCa treatment had always a significantly higher ($p < 0.05$) Y values at 20 °C as compared to 25 °C, resulting in $Y_{25/20}$ ratio < 1 at all incubation times.

The inhibition of Y due to UVA, UVB and UVR at different incubation times is shown in Fig. 3; and it is seen that, in general, HCa had lower inhibition than LCa treatments. However, inhibition of Y due to UVA (Fig. 3a) decreased significantly with time ($p < 0.001$) whereas that due to UVB increased ($p < 0.001$). For UVA-induced inhibition (Fig. 3a) values of ~21–34% were determined after 40 min of exposure whereas they were slightly lower after 80 min (~13–20%) and 2 h (~10–16%). UVB-induced inhibition of Y was higher (i.e., >40%) than that due to UVA and increased with exposure time from values of ~41–50% at 40 min to ~55–60% after 2 h of exposure (Fig. 3b). The UVR-induced inhibition of Y (Fig. 3c) varied from ~71–77% and ~62–74% for LCa and HCa, respectively.

Figure 4 shows the responses of one photoprotective mechanism as assessed through thermal dissipation of excess energy (i.e., non-photochemical quenching, NPQ). The general pattern was of higher NPQ values ($p < 0.05$) with increasing exposure to UVR wavebands, so that those samples receiving UVR wavelengths had higher NPQ than those receiving only PAR. Additionally, and for any radiation treatment, there was a trend for higher NPQ values ($p < 0.05$) at high temperatures, which was especially evident in incubations lasting 80 min (Fig. 4b). Another interesting feature was of higher NPQ values ($p < 0.05$) in HCa than in LCa cells for any radiation treatment at 20 °C; again, this trend was more evident during short time exposures (Fig. 4a) than at the end of the incubation (i.e., after 2 h, Fig. 4c). With increasing exposure time, NPQ

BGD
8, 857–884, 2011

at 25 °C of HCa cells decreased ($p < 0.05$) whereas in LCa increased ($p < 0.05$), so that NPQ differences between the two temperature levels decreased in the HCa-grown cells and increased in the LCa-grown ones, respectively.

3.3 Photosynthetic carbon fixation (*P*), calcification rates (*C*) and *C*/*P*

Photosynthetic carbon fixation of *Emiliania huxleyi* (Fig. 5a) was stimulated by eliminating the shorter wavelengths of the spectrum. The general pattern was of higher photosynthetic carbon values ($p < 0.05$) in the HCa-grown than in the LCa-grown cells. The beneficial effect of temperature was clearly evident in samples acclimated to HCa (Fig. 5a) so that, for example, the highest photosynthetic carbon at 25 °C (Fig. 5a) was 0.76 pg C cell^{-1} h^{-1} whereas at 20 °C was 0.58 pg C cell^{-1} h^{-1}. Under PAR alone (i.e., > 395 nm treatment), however, high temperature significantly inhibited photosynthesis ($p < 0.05$) by 10.1% in the LCa-grown cells. Under UVR, high temperature did not show significant effects on carbon incorporation in the LCa-grown cells. Similar responses were determined in regard to calcification rates (Fig. 5b) with the highest values determined under PAR alone, further benefited by high temperatures especially in the HCa-grown cells, in which calcification rates increased from 0.21 to 0.30 pg C cell^{-1} h^{-1} at 20 and 25 °C, respectively. Calcification rates of LCa were low for all radiation and temperatures treatments. The *C*/*P* ratio of the HCa-grown cells increased slightly with increasing wavelength (Fig. 5c) but there was no clear effect of temperature at both Ca^{2+} concentrations.

Figure 6 shows the relative contribution of UVA and UVB in causing inhibition of photosynthesis, calcification and *C*/*P*. For photosynthesis and calcification, higher inhibition ($p < 0.05$) by UVB as compared to that of UVA was determined. For both Ca^{2+} treatments, however, temperature did not show significant effects on inhibition of photosynthetic carbon fixation and calcification rates ($p > 0.05$, Fig. 6a,b). Finally, UVA induced inhibition of *C*/*P* showed significant ($p < 0.05$) differences among the two Ca^{2+} concentrations (Fig. 6c), but it did not among temperatures. Shorter wavelengths of UVB showed opposite responses: UVB-induced inhibition of *C*/*P* was significantly

BGD
8, 857–884, 2011

different among the two Ca concentrations, being positive for the HCa-grown and negative for the LCa-grown cells, respectively (Fig. 6c). Furthermore, high temperature significantly reduced inhibition of C/P due to UVB ($p < 0.001$, Fig. 6c).

3.4 BWF

There were similar trends of BWFs for inhibition of Y (Fig. 7a), photosynthetic carbon fixation (Fig. 7c) and calcification (Fig. 7d) with decreasing weights towards higher wavelengths. On the other hand, BWFs for inhibition of NPQ (Fig. 7b) showed an opposite response i.e., NPQ was promoted by exposure to short wavelengths. In general, all BWFs did not exhibit significant differences among the two Ca concentrations and the two temperatures tested.

4 Discussion

The results of our study can be summarized as follows: (1) decreased calcification resulted in a decrease of photoprotective mechanisms (NPQ), pigments content and photosynthetic carbon fixation; (2) calcification and photosynthesis (and their ratio) showed different responses related to UVR, with the HCa-grown cells having a better performance as compared to the the LCa-grown ones; (3) elevated temperature increased photosynthesis and calcification of *Emiliania huxleyi*, grown at high Ca^{2+} concentrations whereas the opposite was observed in low Ca^{2+} grown cells. Therefore, a decrease in calcification rates in *E. huxleyi* is expected to decrease photosynthesis rates and also a negative feedback, further reducing calcification.

Emiliania huxleyi depends on Ca^{2+} to form carbonate crystals that build up the coccolith shell that shelters the cells. Ca^{2+} availability is also associated to other process, as seen in other studies (Trimborn et al., 2007; Leonardo et al., 2009) that demonstrated that cells grown under low (0.1 mM Ca^{2+}) or without Ca^{2+} decreased their growth rates as compared to those cultured under higher Ca^{2+} concentrations (e.g.,

BGD
8, 857–884, 2011

1–10 mM). Similarly, in our study we determined a significant decrease in the growth rates of *E. huxleyi* cells after being transferred from 10 mM Ca^{2+} to 0.1 mM Ca^{2+}, but only during the initial 12 generations in 9 days (data not shown). After 100 days (148 generations), there were no significant differences in growth rates between the two Ca^{2+} concentrations (Table 2), clearly suggesting that acclimation to the lowered Ca^{2+} level took longer time than expected (Herfort et al., 2002, 2004; Trimborn et al., 2007; Leonardos et al., 2009). Nevertheless, significant differences between the two Ca^{2+} concentrations were observed in the amount of pigments – chl-*a* and carotenoids per cell (Table 2). The increased contents of the photosynthetic pigments are probably due to the reduced radiation levels received by HCa-grown cells, which had coccolith shelter. In fact, it was previously shown that the coccolith layer reduces the transmission of both UV and PAR, i.e., over 15% of PAR was absorbed by the coccolith layer compared to naked cells (Gao et al., 2009); therefore, LCa-grown cells with less or withouth coccoliths received relatively more radiation. Consequently, the HCa-grown cells upregulated their contents of chl-*a* due to less radiation received, reflecting an increase of the antenna size.

The overall response of *E. huxleyi* cells grown at the high Ca^{2+} concentration and exposed to UVR was of a better performance as compared to those grown at low Ca^{2+} concentration. In addition, elevated temperature enhanced photosynthesis of the HCa-grown cells as compared to the LCa-grown ones (Figs. 2 and 5). There are several mechanisms that might account for part of the observed variations in the responses. For example, dissipation of excess energy as heat (NPQ) is a well known photoprotective mechanism occurring in aquatic photoautotrophs (Falkowski and Raven, 1997). In our case, cells acclimated to HCa had higher NPQ values, at least during short-term incubations, as compared to those under LCa (Fig. 4). Many studies have shown that NPQ and F_v'/F_m' behave as mirror images, with increases in NPQ inversely correlated with decreases in F_v'/F_m' (Adams III and Demmig-Adams, 2004). Carotenoids involved in the xanthophylls cycle may also play an important role in maintaining the energy balance. This cycle has been shown to contribute to photoprotection under visible light

BGD
8, 857–884, 2011

by thermal dissipation of excess excitation energy (Demmig-Adams, 1990). Moreover, while UVR-induced reactive oxygen species (ROS) could damage lipids, DNA and protein (He and Häder, 2002), carotenoids could scavenge singlet oxygen and other ROS (Bornman et al., 1997) thus further allowing cells to reduce or minimize stress. Therefore, it is possible that the higher concentration of carotenoids in the HCa-grown cells might have partially helped them to cope with damaging UVR wavelengths. It is obvious that higher NPQ values coincided with higher calcification rates (Figs. 4 and 5), and overall NPQ values regardless of exposed wavelengths decreased with time (Fig. 4), during which calcification increased (Fig. 5). This implies that calcification plays a role as an alternative way to protect the cells from excessive energy. Reasonably, the processes of calcification and pumping calcium ions consumed additional energy.

After acclimation to the low Ca^{2+} concentration, calcification and photosynthesis at 20 °C decreased by 81.3% and 55.4% (Fig. 5). Other studies (Herfort et al., 2002, 2004; Trimborn et al., 2007; Leonardos et al., 2009) however, found that low Ca^{2+} concentrations did not affect the POC production, photosynthetic carbon fixation or photosynthetic oxygen evolution. In addition, Trimborn et al. (2007) using SEM analysis found naked cells but not coccoliths or even residues, and they concluded that cells did not calcify at 0.1 mM Ca^{2+} concentrations. In general, it can be considered that calcite dissolution occurs when the calcite saturation state (Ω) is < 1 (Trimborn et al., 2007). In our study, and although some part of the coccolith layer dissolved under the calcium carbonate undersaturated conditions ($\Omega < 0.1$), our SEM analysis of the LCa-grown cells showed that they did not loose the capacity to produce coccoliths (Fig. 1). It is known that photosynthesis drives calcification by providing the energy required to transport inorganic carbon and calcium ions and to accumulate them inside the coccolith producing vesicle (Brownlee and Taylor, 2004). In the case of our LCa cells, calcification decreased to 18.7% as compared to cells grown at ambient Ca^{2+} concentration (HCa, Fig. 5). Therefore, the LCa-grown cells might not need energy as much as the HCa-grown cells do to calcify due to reduced availability of Ca^{2+}, then photosynthetic activity, as reflected by the lower Y and carbon fixation rates, were

BGD
8, 857–884, 2011

down-regulated. This is well consistent with the fact that no difference in the growth rate was found between the LCa-grown and the HCa-grown cells (Table 2), which reflected the net energy balance.

Cells grown at LCa and HCa displayed significant differences in the inhibition of C/P (Figs. 5–7). Moreover, the responses of photosynthesis and calcification towards UVR appear to be not synchronous. In this sense, Paasche (1966) found that calcification and photosynthesis of *Emiliania huxleyi* had different action spectra, as for example blue light appeared to be more efficient in calcification than in photosynthetic carbon fixation. In our study, and in agreement with a previous work (Gao et al., 2009), we showed no UVA impact on the C/P ratio of *E. huxleyi* but a significant UVB-induced decrease of C/P. However, some differences might arise when considering the responses on more dense cultures (Guan and Gao, 2010) with shorter wavelengths of UVB causing more damage to photosynthesis than to calcification, and longer wavelengths of UVA resulting in a decrease of calcification; in general terms, large cell density affects the control of the carbonate system (Gattuso et al., 2010). In addition, senescent and nutrient-limited cells tend to acquire extra layers of coccoliths (Paasche, 2002; Shiraiwa, 2003). Furthermore, and as previously mentioned, the coccolith layer around the cell surface could effectively reduce the transmission of UV-B (Gao et al., 2009).

The observed increase in photosynthesis of HCa cells under high temperature (Fig. 5) was similar to the results obtained by Feng et al. (2008). Photosynthetic carbon fixation is largely controlled by enzymes related to dark reactions (Falkwoski and Raven, 1997) and so its rate should also be temperature-dependent, with the enzymes involved in photosynthetic carbon fixation and calcification being stimulated by high temperatures. Additionally, some enzymes in *E. huxleyi* such as phosphatase were affected by reduced Ca^{2+} concentrations (Shaked et al., 2006). Thus, if the enzymes of *E. huxleyi* were affected by long time acclimation to low Ca^{2+} concentration, this may have contributed to the different response of photosynthesis and calcification between two experimental Ca^{2+} concentrations (Fig. 5). Moreover, McNeil et al. (2004)

BGD
8, 857–884, 2011

have suggested that the average annual coral calcification rate will increase in a future ocean warming scenario, though decreased calcification of the Great Barrier Reef was suggested to link to global warming and ocean acidification (De'ath et al., 2009). In fact in our study, the calcification of *E. huxleyi* significantly increased at high temperatures (Fig. 5). However, Feng et al. (2008) did not observe such a significant effect of elevated temperature on calcification of this coccolithophore. Moreover, a 5 °C increase in temperature (from 13 to 18 °C) decreased the calcification rate of *E. huxleyi* grown at both, present and future CO_2 concentrations (De Bodt et al., 2010). It is likely that the differential responses of photosynthesis and calcification at different levels of temperature are responsible for such discrepancies, since photosynthetic carbon fixation process could be more sensitive to temperature as compared to calcification in this species. However, it can not be ruled out that specific responses among different strains, or counteracting effects due to differences in pH are also responsible for differences in responses even within the same species.

The ongoing ocean acidification is compounded with the shoaling of the mixed layer, increased surface seawater temperature and increased exposures of the cells to high radiation levels. Our results indicate that reduced calcification in *E. huxleyi* made the cells more vulnerable when they are exposed to excessive light energy even without UVR considered, since reduced calcification led to down-regulated photoprotective capability. In addition, increased temperature decreased the C/P ratio in the LCa-grown cells. Combined with the previous finding that reduced calcification led to enhanced sensitivity to UVR and decreased ratio of C/P (Gao et al., 2009), the combined effects of ocean acidification, global warming and increased light and UV exposures will synergistically reduce the C/P ratio, which would eventually affect the carbon-related biogeochemical processes.

BGD
8, 857–884, 2011

Acknowledgements. This study was supported by National Basic Research Program of China (No. 2009CB421207), by program for Changjiang Scholars and Innovative Research Team (IRT0941) and by National Natural Science Foundation (No. 40930846, No. 40876058). VEV and EWH were supported by the Visiting Professor Program (111) from the Ministry of Education of China. This is Contribution No. 123 of Estación de Fotobiología Playa Unión.

References

Adams III, W. W. and Demmig-Adams, B.: Chlorophyll fluorescence as a tool to monitor plant response to the environment, in: Chlorophyll-*a* Fluorescence: a Signature of Photosynthesis, edited by: Papageorgiou, G. C. and Govindjee: Springer, Berlin, Germany, 583–604, 2004.

Anning, T., Nimer, N., Merrett, M. J., and Brownlee, C.: Costs and benefits of calcification in coccolithophorids, J. Marine Syst., 9, 45–56, 1996.

Beardall, J., Sobrino, C., and Stojkovic, S.: Interactions between the impacts of ultraviolet radiation, elevated CO_2, and nutrient limitation on marine primary producers, Photochem. Photobiol. S., 8, 1257–1265 doi:10.1039/b9pp00034h, 2009.

Bornman, J. F., Reuber, S., Cen, Y., and Weissenböck, G.: Ultraviolet radiation as a stress factor and the role of protective pigments, in: Plants and UV-B: Responses to Environmental Change, edited by: Lumsden, P. J., Cambridge University Press, Cambridge, NY, 157–168, 1997.

Brownlee, C. and Taylor, A.: Calcification in coccolithophores: a cellular perspective, in: *Coccolithophores*: from Molecular Biology to Global Impact, edited by: Thierstein, H. R. and Young, J. R., Springer, Berlin, Germany, 31–49, 2004.

Brownlee, C., Davies, M., Nimer, N., Dong, L., and Merrett, M.: Calcification, photosynthesis and intracellular regulation in *Emiliania huxleyi*, B. Inst. Oceanogr. Monaco, 14, 19–35, 1995.

Buma, A. G. J., van Oijen, T., van de Poll, W., Veldhuis, M. J. W., and Gieskes, W. W. C.: The sensitivity of *Emiliania huxleyi* (*Prymnesiophyceae*) to ultraviolet-B radiation, J. Phycol., 36, 296–303, 2000.

Cokacar, T., Kubilay, N., and Oguz, T.: Structure of *Emiliania huxleyi* blooms in the Black Sea surface waters as detected by SeaWIFS imagery, Geophys. Res. Lett., 28, 4607–4610, 2001.

BGD

8, 857–884, 2011

De'ath, G., Lough, J. M., and Fabicius, K. E.: Declining coral calcification on the Great Barrier Reef, Science, 323, 116–119, 2009.
De Bodt, C., Van Oostende, N., Harlay, J., Sabbe, K., and Chou, L.: Individual and interacting effects of pCO_2 and temperature on *Emiliania huxleyi* calcification: study of the calcite production, the coccolith morphology and the coccosphere size, Biogeosciences, 7, 1401–1412, doi:10.5194/bg-7-1401-2010, 2010.
Demmig-Adams, B.: Carotenoids and photoprotection in plants: a role for the xanthophylls zeaxanthin, Biochim. Biophys. Acta, 1020, 1–24, 1990.
Dickson, A. G. and Millero, F. J.: A comparison of the equilibrium constants for the dissociation of carbonic acid in seawater media, Deep-Sea Res., 34, 1733–1743, 1987.
Falkowski, P. G. and Raven, J. A.: Aquatic Photosynthesis, Blackwell Scientific, Oxford, UK, 1997.
Feng, Y., Warner, M. E., Zhang, Y., Sun, J., Fu, F., Rose, J. M., and Hutchins, D. A.: Interactive effects of increased pCO_2, temperature and irradiance on the marine coccolithophore *Emiliania huxleyi* (*Prymnesiophyceae*), Eur. J. Phycol., 43, 87–98, 2008.
Gao, K., Ruan, Z., Villafañe, V. E., Gattuso, J. P., and Helbling, E. W.: Ocean acidification exacerbates the effect of UV radiation on the calcifying phytoplankter *Emiliania huxleyi*, Limnol. Oceanogr., 54, 1855–1862, 2009.
Genty, B. E., Briantais, J. M., and Baker, N. R.: Relative quantum efficiencies of the two photosystems of leaves in photorespiratory and non-photorespiratory conditions, Plant Physiol. Bioch., 28, 1–10, 1989.
Guan, W. and Gao, K.: Impacts of UV radiation on photosynthesis and growth of the coccolithophore *Emiliania huxleyi* (*Haptophyceae*), Environ. Exp. Bot., 67, 502–508, 2010.
Gattuso, J. P., Gao, K., Lee, K., Rost, B., and Schulz, K. G.: Approaches and tools to manipulate the carbonate chemistry, in: Guide to Best Practices for Ocean Acidification Research and Data Reporting, edited by: Riebesell, U., Fabry, V. J., Hansson, L., and Gattuso, J.-P., Publications Office of the European Union, Luxembourg, 41–52, 2010.
He, Y. and Häder, D. P.: Reactive oxygen species and UV-B: effects on cyanobacteria, Photochem. Photobiol. S., 1, 729–736, 2002.
Herfort, L., Thake, B., and Roberts, R. J.: Acquisition and use of bicarbonate by *Emiliania huxleyi*, New Phytol., 156, 427–436, 2002.
Herfort, L., Loste, E., Meldrum, F., and Thake, B.: Structural and physiological effects of calcium and magnesium in *Emiliania huxleyi* (Lohmann) Hay and Mohler, J. Struct. Biol., 148,

BGD
8, 857–884, 2011

307–314, 2004.
Leonardos, N., Read, B., Thake, B., and Young, J. R.: No mechanistic dependence of photosynthesis on calcification in the coccolithophorid *Emiliania huxleyi* (*Haptophyta*), J. Phycol., 45, 1046–1051. 2009.
Lewis, E. and Wallace, D. W. R.: Program Developed for CO_2 System Calculations, ORNL/CDIAC-105, Carbon Dioxide Information Analysis Center, Oak Ridge National Laboratory, US Department of Energy, Oak Ridge, Tennessee, 1998.
McNeil, B. I., Matear, R. J., and Barnes, D. J.: Coral reef calcification and climate change: the effect of ocean warming, Geophys. Res. Lett., 31, L22309, doi:10.1029/2004GL021541, 2004.
Mehrbach, C., Culberson, C. H., Hawley, J. E., and Pytkowicz, R. N.: Measurement of the appearent dissociation constants of carbonic acid in seawater at atmospheric pressure, Limnol. Oceanogr., 18, 897–907, 1973.
Milliman, J. D.: Production and accumulation of calcium carbonate in the ocean: budget of a nonsteady state, Global Biogeochem. Cy., 7, 927–957, 1993.
Neale, P. J. and Kieber, D. J.: Assessing biological and chemical effects of UV in the marine environment: spectral weighting functions, in: Causes and Environmental Implications of Increased UV-B Radiation, edited by: Hester, R. E. and Harrison, R. M., The Royal Society of Chemistry, Cambridge, 61–83, 2000.
Nanninga, H. J. and Tyrrell, T.: Importance of light for the formation of algal blooms by *Emiliania huxleyi*, Mar. Ecol.-Progr. Ser., 136, 195–203, 1996.
Nimer, N. A., Merrett, M. J., and Brownlee, C.: Inorganic carbon transport in relation to culture age and inorganic carbon concentration in a high calcifying strain of *Emiliania huxleyi*, J. Phycol., 32, 813–818, 1996.
Paasche, E.: Action spectrum of coccolith formation, Physiol. Plantarum, 19, 770–779, 1966.
Paasche, E.: A review of the coccolithophorid *Emiliania huxleyi* (*Prymnesiophyceae*), with particular reference to growth, coccolith formation, and calcification photosynthesis interactions, Phycologia, 40, 503–529, 2002.
Porra, R. J.: The chequered history of the development and use of simultaneous equations for the accurate determination of chlorophylls a and b, Photosynth. Res., 73, 149–156, 2002.
Rost, B. and Riebesell, U.: *Coccolithophores* and the biological pump: responses to environmental changes, in: *Coccolithophores*: from Molecular Biology to Global Impact, edited by: Thierstein, H. R. and Young, J. R., Springer, Berlin, Germany, 76–99, 2004.

BGD
8, 857–884, 2011

Shaked, Y., Xu, Y., Leblanc, K., and Morel, F. M. M.: Zinc availability and alkaline phosphatase activity in *Emiliania huxleyi*: implications for Zn-P co-limitation in the ocean, Limnol. Oceanogr., 51, 299–309, 2006.

Shiraiwa, Y.: Physiological regulation of carbon fixation in the photosynthesis and calcification of coccolithophorids, Comp. Biochem. Phys. B, 136, 775–783, 2003

Sikes, C. S. and Wilbur, K. M.: Function of coccolith formation, Limnol. Oceanogr., 27, 18–26, 1982.

Sikes, C. S., Roer, R. D., and Wilbur, K. M.: Photosynthesis and coccolith formation: inorganic carbon sources and net inorganic reaction of deposition, Limnol. Oceanogr., 25, 248–261, 1980.

Strickland, J. D. H. and Parsons, T. R.: A practical handbook of seawater analysis, B. Fish. Res. Board Can., 167, 49–80, 1972.

Sunda, W. G., Price, N. M., and Morel, F. M. M.: Trace metal ion buffers and their use in culture studies, in: Algal Culturing Techniques, edited by: Andersen, R. A., Elsevier Academic Press, New York, 2005.

Trimborn, S., Langer, G., and Rost, B.: Effect of varying calcium concentrations and light intensities on calcification and photosynthesis in *Emiliania huxleyi*, Limnol. Oceanogr., 52, 2285–2293, 2007.

Villafañe, V. E., Sundbäck, K., Figueroa, F. L., and Helbling, E. W.: Photosynthesis in the aquatic environment as affected by UVR, in: UV Effects in Aquatic Organisms and Ecosystems, edited by: Helbling, E. W. and Zagarese, H. E., The Royal Society of Chemistry, Cambridge, 357–397, 2003,

Zondervan, I.: The effects of light, macronutrients, trace metals and CO_2 on the production of calcium carbonate and organic carbon in coccolithophores – a review, Deep-Sea Res. Pt. II, 54, 521–537, 2007.

BGD

8, 857–884, 2011

Table 1. Parameters of the artificial seawater carbonate system at the ambient (10 mM) and reduced (0.1 mM) levels of Ca^{2+} equilibrated with ambient CO_2 (39.3 Pa). Total alkalinity, pH, salinity, nutrient concentration and temperature were used to derive all other parameters using a CO_2 system analyzing software (CO_2SYS). Data are the means ± SD of 3 measurements.

Ca^{2+} (mM)	pH_{NBS}	TA (µmol kg^{-1})	pCO_2 (ppmV)	DIC (µmol kg^{-1})	CO_2 (μmo kg^{-1})	HCO_3^- (µmol kg^{-1})	CO_3^{2-} (µmol kg^{-1})
10	8.20 ± 0.01	2539 ± 12*	405 ± 6	2238 ± 11	13 ± 0.2	2008 ± 10	216 ± 3*
0.1	8.20 ± 0.01	2496 ± 24*	405 ± 15	2202 ± 28	13 ± 0.5	1979 ± 29	210 ± 2*

* The asterisks denote significant difference between the two Ca^{2+} concentrations.

BGD
8, 857–884, 2011

Table 2. Growth rate (in d^{-1}), chl-*a* and carotenoid content (in pg $cell^{-1}$) of *Emiliania huxleyi* cells acclimated to 10 mM (HCa) or 0.1 mM Ca^{2+} (LCa) for at least 148 generations.

Variable	Ca^{2+} (mM)		*p*
	10	0.1	
Specific growth rate (d^{-1})	1.07 ± 0.04 ($n = 14$)	1.03 ± 0.05 ($n = 10$)	$p > 0.05$
Chl-*a* (pg $cell^{-1}$)	0.15 ± 0.01 ($n = 6$)*	0.11 ± 0.01 ($n = 6$)	$p < 0.001$
Carotenoids (pg $cell^{-1}$)	0.30 ± 0.02 ($n = 6$)*	0.24 ± 0.02 ($n = 6$)	$p < 0.01$

n represents the number of samples.
* The asterisks represent significant differences between two Ca^{2+} concentrations.

BGD
8, 857–884, 2011

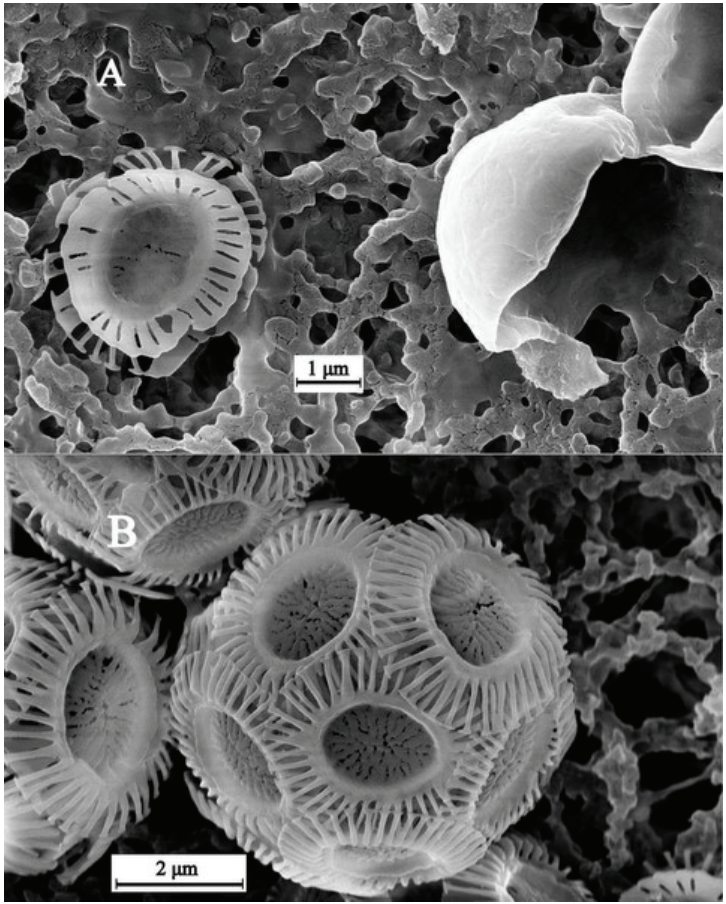

Fig. 1. Scanning electron microscope images of *Emiliania huxleyi* cells grown at: **(A)** 0.1 mM Ca^{2+}, and **(B)** 10 mM Ca^{2+} grown at 20 °C and under PAR illumination of 150 µmol m^{-2} s^{-1}.

BGD
8, 857–884, 2011

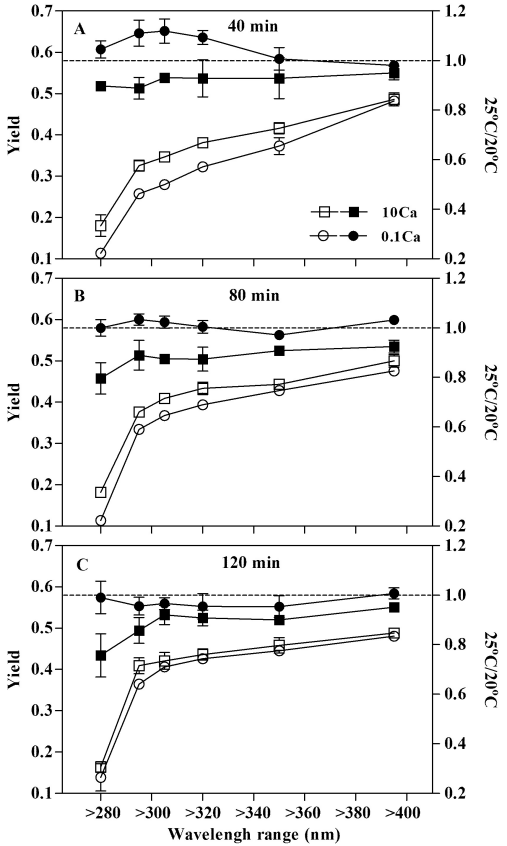

Fig. 2. Effective photochemical quantum yield (F_v'/F_m') of *Emiliania huxleyi* cells grown at HCa (squares) and LCa (circles). Open symbols indicate F_v'/F_m' measured at 20 °C whereas black symbols indicate the ratio of F_v'/F_m' measured at 25 °C to that at 20 °C. Measurements done after exposures of: **(A)** 40 min, **(B)** 80 min and, **(C)** 120 min. The bars on top of the symbols represent the standard deviation ($n = 3$).

BGD
8, 857–884, 2011

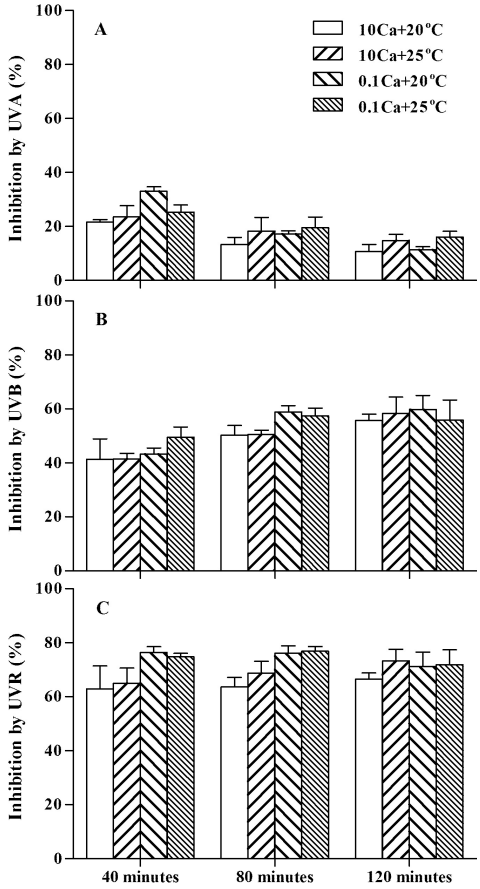

Fig. 3. Inhibition of the effective photochemical quantum yield of *Emiliania huxleyi* cells due to: **(A)** UVA, **(B)** UVB, and **(C)** UVR after 40, 80 and 120 min of exposure to artificial radiation. The lines on top of the bars represent the standard deviations ($n = 3$).

BGD
8, 857–884, 2011

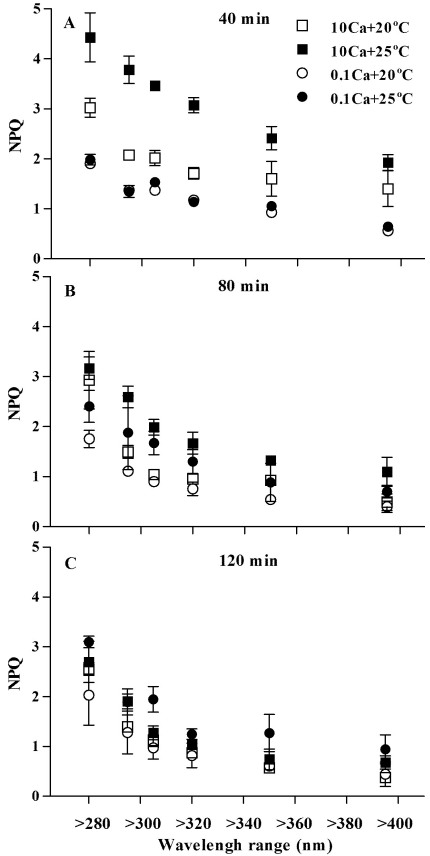

Fig. 4. Non photochemical quenching (NPQ) of *Emiliania huxleyi* cells grown at HCa (squares) and LCa (circles) and exposed to different radiation and temperature treatments. Open and filled symbols are cells exposed at 20 °C and 25 °C, respectively. Measurements done after exposures of: **(A)** 40 min, **(B)** 80 min, and **(C)** 120 min. The bars on top of the symbols represent the standard deviation ($n = 3$).

BGD
8, 857–884, 2011

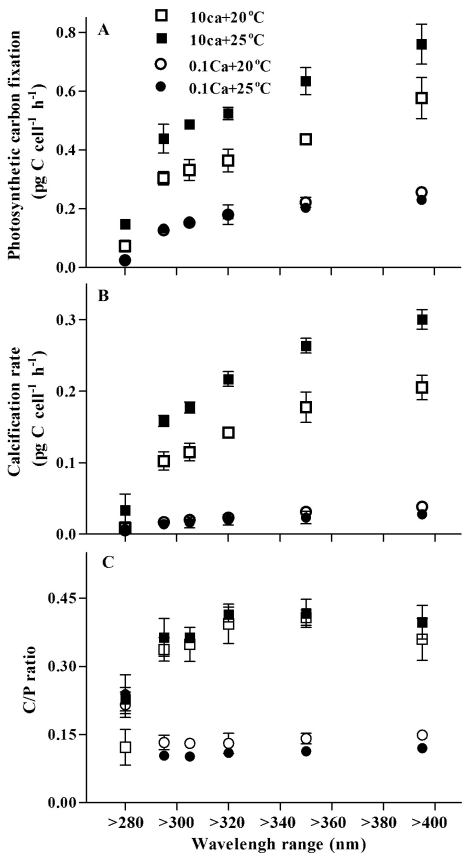

Fig. 5. **(A)** Photosynthetic carbon fixation (in pg C cell^{-1} h^{-1}), **(B)** calcification rate (in pg C cell^{-1} h^{-1}), and **(C)** *C*/*P* ratio of *Emiliania huxleyi* cells grown at HCa (squares) and LCa (circles) and exposed to different radiation and temperature treatments for 2 h. Open and filled symbols are cells exposed at 20 °C and 25 °C, respectively. The bars on top of the symbols represent the standard deviation ($n = 3$).

BGD
8, 857–884, 2011

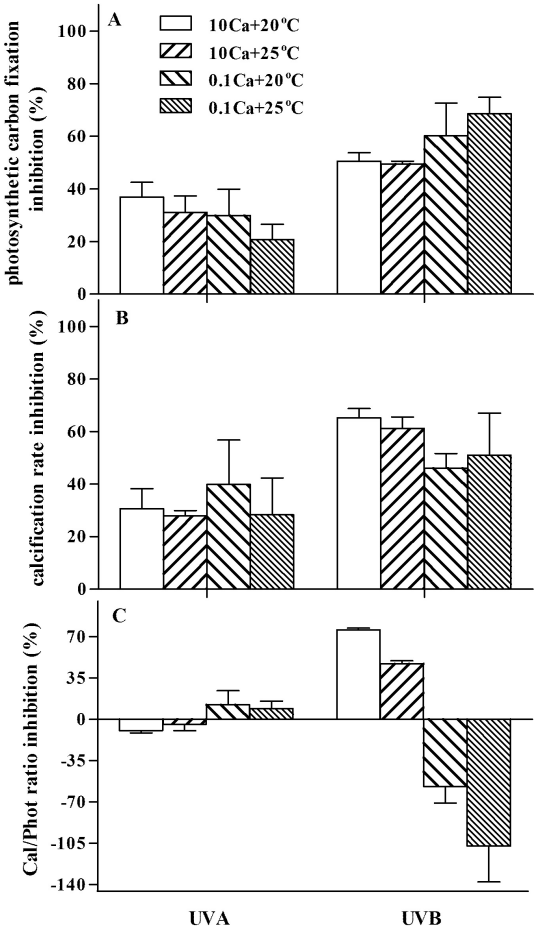

Fig. 6. UVR-induced inhibition of **(A)** photosynthetic carbon fixation, **(B)** calcification rate and, **(C)** *C*/*P* ratio of *Emiliania huxleyi* cells. The lines on top of the bars represent the standard deviations ($n = 3$).

BGD
8, 857–884, 2011

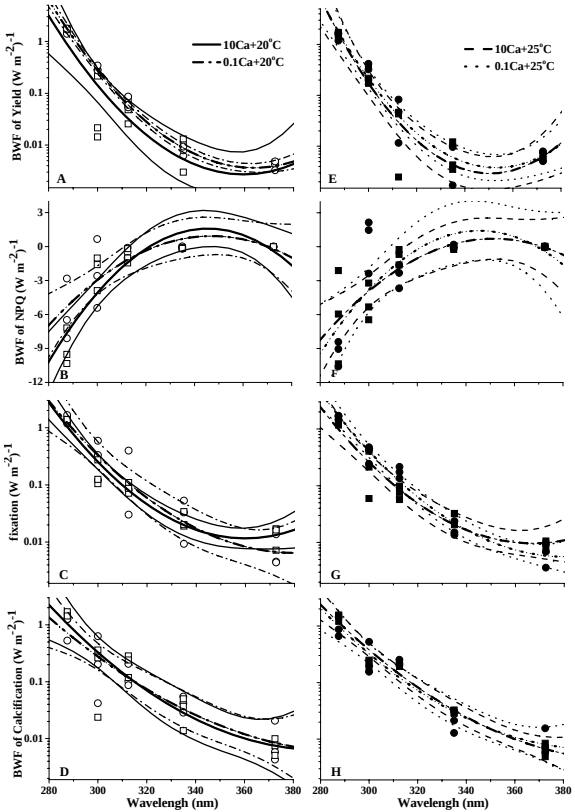

Fig. 7. Biological weighting functions (BWFs, in $(W\ m^{-2})^{-1}$) of *Emiliania huxleyi*: **(A)** effective photochemical quantum yield (Y); **(B)** non photochemical quenching (NPQ); **(C)** photosynthetic carbon fixation and, **(D)** calcification rate of cells grown at HCa and LCa concentrations. The symbols represent the different combinations of Ca^{2+} concentration and temperature: open squares: HCa cells at 20 °C; filled squares: HCa cells at 25 °C; open circles: LCa cells at 20 °C and filled circles: LCa cells at 25 °C.

BGD
8, 857–884, 2011